RINGWOOD, A. E., KESSON, S. E. & WARE, N. G. (1980). *Sci. Basis Nucl. Waste Manage.* **2**, 265–272.
RINGWOOD, T. (1982). *Am. Sci.* **70**, 201–207.
RUSSELL, L. E., HARRISON, J. D. L. & BRETT, N. H. (1960). *J. Nucl. Mater.* **2**, 310–320.
SCOTT, J. F. (1974). *Rev. Mod. Phys.* **46**, 83–128.
SEARS, V. F. (1986). *Methods Exp. Phys.* **23A**, 521–550.
SHANNON, R. D. (1976). *Acta Cryst.* A**32**, 751–767.
VON DREELE, R. B. (1984). Personal communication.
VON DREELE, R. B., JORGENSEN, J. D. & WINDSOR, C. G. (1982). *J. Appl. Cryst.* **15**, 581–589.
WILLIAMS, C. W., MORSS, L. R. & CHOI, I. (1984). *Am. Chem. Soc. Symp. Ser.* No. 246, edited by G. S. BARNEY, J. D. NAVRATIL & W. W. SCHULTZ, pp. 323–334. Washington, DC: American Chemical Society.
WINDSOR, C. G. (1981). *Pulsed Neutron Scattering.* New York: Halsted Press.
ZACHARIASEN, W. H. (1978). *J. Less-Common Met.* **62**, 1–7.

Acta Cryst. (1988). B**44**, 580–585

Electron-Density Distribution in Crystals of Dipotassium Tetrachloropalladate(II) and Dipotassium Hexachloropalladate(IV), $K_2[PdCl_4]$ and $K_2[PdCl_6]$ at 120 K

BY HIROYUKI TAKAZAWA, SHIGERU OHBA AND YOSHIHIKO SAITO

Department of Chemistry, Faculty of Science and Technology, Keio University, Hiyoshi 3, Kohoku-ku, Yokohama 223, Japan

(*Received 1 June* 1988; *accepted 9 August* 1988)

Abstract

Mo $K\alpha_1$, $\lambda = 0·70926$ Å, $T = 120\,(2)$ K. (I): $K_2[PdCl_4]$, $M_r = 326·4$, tetragonal, $P4/mmm$, $a = 7·0259\,(3)$, $c = 4·0797\,(2)$ Å, $V = 201·39\,(2)$ Å^3, $Z = 1$, $D_x = 2·69$ Mg m^{-3}, $\mu = 4·55$ mm^{-1}, $F(000) = 151·7$, final $R = 0·021$ for 893 unique reflections. (II): $K_2[PdCl_6]$, $M_r = 397·3$, cubic, $Fm3m$, $a = 9·6374\,(4)$ Å, $V = 895·12\,(7)$ Å^3, $Z = 4$, $D_x = 2·95$ Mg m^{-3}, $\mu = 4·71$ mm^{-1}, $F(000) = 744·0$, final $R = 0·011$ for 393 unique reflections. The Pd—Cl bond lengths are 2·3066 (2) and 2·3094 (3) Å for (I) and (II), respectively. The asphericity of the 4*d* electron distribution in the square-planar and octahedral Pd complexes could be detected clearly. Above and below the $[PdCl_4]^{2-}$ plane of (I), excess densities of 2·3 (3) e Å^{-3} are found at 0·47 Å from the Pd nucleus, suggesting enhancement of the d_{z^2} orbital population. In (II), positive deformation densities corresponding to the t_{2g} orbitals are observed in the [111] directions at 0·5 Å from the Pd nucleus and 1·4 (3) e Å^{-3} in height. These charge asphericities could be reproduced by the multipole expansion method with reasonable *d*-orbital populations.

Introduction

Since Iwata & Saito (1973) reported the aspherical distribution of the 3*d* electrons in $[Co(NH_3)_6][Co(CN)_6]$, a number of studies on transition metals and their complexes have been performed (Coppens & Hall, 1982; Toriumi & Saito, 1983). Preliminary papers on $K_2[PtCl_4]$ (Ohba, Sato, Saito, Ohshima & Harada, 1983) and $K_2[PtCl_6]$ (Ohba & Saito, 1984) suggested that even 5*d* electrons may be detected in spite of a very small valence/total electron ratio. Before exploring further the asphericity of 5*d* electrons in a ligand field, the isomorphous Pd complexes involving 4*d* electrons were examined in the present study.

Experimental

(I): Dark-green needle-like crystals were grown from an aqueous solution of $PdCl_2$ and KCl. A crystal was shaped into a sphere of 0·378 (5) mm in diameter and cooled with a stream of cold nitrogen gas. Intensities were measured on a Rigaku AFC-5 automated four-circle diffractometer with graphite-monochromatized Mo $K\alpha$ radiation, θ–2θ scan technique with scan speed 6° min^{-1} in θ and scan width $(1·4 + 0·36\tan\theta)°$. Range of indices, $-12 \le h,\ k \le 12,\ 0 \le l \le 7$ $(0 < 2\theta \le 80°)$; $-17 \le h \le 17,\ 0 \le k \le 17,\ 0 \le l \le 9$ $(80 < 2\theta \le 120°)$. Standard reflections varied within 3%, 4753 reflections were measured; 4387 reflections observed with $|F_o| > 3\sigma(|F_o|)$; 893 unique reflections $(R_{\rm int} = 0·016)$. Lattice constants were based on 20 2θ values $(60 < 2\theta < 76°)$. Correction for absorption made with $\mu r = 0·860$ $(0·293 < A < 0·351)$. Conventional refinement performed by the full-matrix least-squares program *RADIEL* (Coppens, Guru Row, Leung, Stevens, Becker & Yang, 1979). Function $\sum w(|F_o| - |F_c|)^2$ minimized with weight $w^{-1} = \sigma^2(|F_o|) + (0·015|F_o|)^2$. Introducing an isotropic secondary-extinction correction parameter (Zachariasen, 1967), $g = 0·14\,(1) \times 10^{-4}$, reduced R from 0·030 to 0·021 for 893 unique reflections. $wR = 0·036$, $S = 1·9$, reflection/parameter = 81·2, $\Delta/\sigma < 0·2$. Complex neutral-atom scattering factors were taken from *International Tables for X-ray Crystallography* (1974). Calculations were carried out on a FACOM M-380R computer of this university.

0108-7681/88/060580-06$03.00

Table 1. *Positional* ($\times 10^5$) *and thermal* ($\times 10^5$ Å^2) *parameters*

The thermal parameters are expressed as follows: $\exp[-2\pi^2(h^2a^{*2}U_{11} + k^2b^{*2}U_{22} + l^2c^{*2}U_{33} + 2hka^*b^*U_{12})]$. First row: conventional refinement; second row: multipole refinement [the result of the refinement *C* for (I)]. Only conventional refinement was performed for the room-temperature data.

	x	y	z	U_{11} or $U_{\rm iso}$	U_{22}	U_{33}	U_{12}
(I) at 120 K							
Pd	0	0	0	788 (5)	($=U_{11}$)	1042 (6)	
	0	0	0	765 (6)	($=U_{11}$)	1006 (8)	
Cl	23214 (3)	($=x$)	0	1101 (7)	($=U_{11}$)	1940 (14)	−147 (7)
	23213 (3)	($=x$)	0	1095 (8)	($=U_{11}$)	1950 (14)	−132 (7)
K	0	50000	50000	2762 (23)	1275 (14)	1175 (13)	
	0	50000	50000	2730 (23)	1270 (14)	1191 (13)	
(I) at 294 K							
Pd	0	0	0	1886 (3)	($=U_{11}$)	2296 (5)	
Cl	23066 (2)	($=x$)	0	2498 (5)	($=U_{11}$)	4232 (10)	−353 (5)
K	0	50000	50000	5726 (20)	2848 (11)	2706 (10)	
(II) at 120 K							
Pd	0	0	0	520 (3)			
	0	0	0	503 (4)			
Cl	23963 (3)	0	0	639 (7)	1568 (7)	($=U_{22}$)	
	23962 (2)	0	0	648 (6)	1557 (6)	($=U_{22}$)	
K	25000	25000	25000	1350 (6)			
	25000	25000	25000	1351 (6)			
(II) at 299 K							
Pd	0	0	0	1416 (5)			
Cl	23795 (5)	0	0	1569 (12)	3938 (17)	($=U_{22}$)	
K	25000	25000	25000	3560 (17)			

Multipole refinement carried out with the program *MOLLY* (Hansen & Coppens, 1978). Multipoles included up to hexadecapole for both the Pd and Cl atoms. The Pd and Cl atoms lie on the site symmetry $4/mmm$ and $mm2$, and the number of multipole parameters is four and nine for Pd and Cl atoms, respectively. For the Pd atom the x and y axes of the multipole functions were along the Pd—Cl bond directions, with z along the fourfold axis. The radial functions were $r^{n_l}\exp(-\zeta r)$ with $n_l = 4$ for any value of l. An isotropic extinction parameter of type I with Lorentzian distribution was introduced (Becker & Coppens, 1975). The core and valence scattering factors of Pd and Cl and the scattering factors of the K^+ ion were from *International Tables for X-ray Crystallography* (1974), with core electron configurations for Pd and Cl atoms assumed to be Kr and Ne, respectively. The charge of the unit cell was constrained to be zero with a fixed single positive charge for K^+. The positional, thermal, multipole and radial parameters, κ (Coppens *et al.*, 1979), were refined based on all the observed unique reflections. Initial ζ values were 4·4 Å^{-1} for Pd^{2+} (Eyring, Walter & Kimball, 1944) and 4·0 Å^{-1} for Cl (Clementi & Raimondi, 1963). When the ζ(Pd) was refined to be 5·2 (3) Å^{-1}, the R value reduced from 0·021 to 0·020. ζ(Cl), which could not be refined successfully, was fixed at the value of 4·0 Å^{-1}. The refined populations for the $a_{1g}(d_{z^2})$ and $e_g(d_{xz}, d_{yz})$ orbitals, 2·41 (5) and 4·49 (6) (refinement *A*), violated Pauli's exclusion principle. Thereafter, they were fixed at two and four. Furthermore the population of the $b_{2g}(d_{xy})$ orbital became 2·25 (3) [$R = 0{\cdot}021$, $\zeta(\mathrm{Pd}) = 7{\cdot}5$ (9): refinement *B*]. This was then fixed at two (refinement *C*). Final $R = 0{\cdot}021$, $wR = 0{\cdot}034$, $S = 1{\cdot}82$, $g = 1{\cdot}6\ (1) \times 10^{-4}$ and $y_{\rm min} = 0{\cdot}53$ for 220. $\kappa(\mathrm{Pd}) = 1{\cdot}12$ (1), $\kappa(\mathrm{Cl}) = 1{\cdot}04$ (1), $\zeta(\mathrm{Pd}) = 7{\cdot}3$ (10), $\Delta/\sigma < 0{\cdot}1$, reflection/parameter = 37·2.*

(II): Purple–red crystals showing the forms {111} and {100} were grown from mixture of $PdCl_2$ and KCl aqueous solutions and aqua regia. A spherically ground crystal 0·354 (8) mm in diameter was used in the intensity measurements. Range of indices, $-13 \le h, k \le 13$, $0 \le l \le 13$ ($0 < 2\theta \le 60°$), and $0 \le h, k, l \le 23$ ($60 < 2\theta \le 120°$). Variation of standards within 1%, 2896 reflections measured, 2856 reflections observed, 393 unique ($R_{\rm int} = 0{\cdot}013$). After absorption correction with $\mu r = 0{\cdot}833$ ($0{\cdot}304 < A < 0{\cdot}360$), a conventional refinement was carried out with *RADIEL*. The correction for isotropic secondary extinction, $g = 0{\cdot}084\ (7) \times 10^{-4}$, reduced R from 0·022 to 0·013 for 393 unique reflections. $wR = 0{\cdot}019$, $S = 1{\cdot}1$, reflection/parameter = 56·1, $\Delta/\sigma < 0{\cdot}01$. Multipole refinement was carried out with *MOLLY*. The number of population parameters of the multipoles for the Pd and Cl atoms are two and six corresponding to the site symmetries $m3m$ and $4mm$, respectively. ζ(Cl) was fixed at 4·0 Å^{-1}. Final $R = 0{\cdot}011$, $wR = 0{\cdot}016$ and $S = 0{\cdot}94$ for 393 unique reflections, $g = 0{\cdot}087\ (6) \times 10^{-4}$ and $y_{\rm min} = 0{\cdot}64$ for 400. $\kappa(\mathrm{Pd}) = 1{\cdot}09$ (2), $\kappa(\mathrm{Cl}) = 1{\cdot}02$ (1), $\zeta(\mathrm{Pd}) = 5{\cdot}7$ (2) Å^{-1}, $\Delta/\sigma < 0{\cdot}1$, reflection/parameter = 21·8.*

---

* Lists of structure factors, multipole parameters, and figures of observed deformation densities at room temperature and model deformation densities have been deposited with the British Library Document Supply Centre as Supplementary Publication No. SUP 51225 (46 pp.). Copies may be obtained through The Executive Secretary, International Union of Crystallography, 5 Abbey Square, Chester CH1 2HU, England.

Intensities were also measured for (I) and (II) at room temperature. (I): $a = 7{\cdot}0673$ (2), $c = 4{\cdot}1258$ (2) Å, $V = 206{\cdot}07$ (1) Å^3, $T = 294$ (1) K, $D_x = 2{\cdot}64$ Mg m^{-3}, $\mu = 4{\cdot}44$ mm^{-1}, $2\theta_{\max}$(Mo $K\alpha$) = 100° with θ–2θ scan. Spherical crystal 0·41 (2) mm in diameter. 4666 reflections measured, 4230 reflections observed, 675 unique ($R_{\rm int} = 0{\cdot}013$). Conventional refinement was made with *RADIEL*. Final $R = 0{\cdot}020$, $wR = 0{\cdot}028$, $S = 1{\cdot}2$, $y_{\min} = 0{\cdot}34$ for 220, Pd—Cl = 2·3054 (2) Å. (II): $a = 9{\cdot}7097$ (3) Å, $V = 915{\cdot}41$ (4) Å^3, $T = 299$ (1) K, $D_x = 2{\cdot}88$ Mg m^{-3}, $\mu = 4{\cdot}61$ mm^{-1}, $2\theta_{\max}$(Mo $K\alpha$) = 120° with θ–2θ scan. The specimen was that for the low-temperature work. 5090 reflections measured, 4623 reflections observed, 400 unique ($R_{\rm int} = 0{\cdot}020$). Final $R = 0{\cdot}018$, $wR = 0{\cdot}026$, $S = 1{\cdot}3$, $y_{\min} = 0{\cdot}71$ for 400, Pd—Cl = 2·3103 (5) Å.*

Results and discussion

Atomic parameters are given in Table 1. Deformation densities were calculated based on all the observed unique reflections ($\sin\theta/\lambda \le 1{\cdot}22$ Å^{-1}) after anomalous-dispersion correction on the basis of equation (3) below, where the structure factors were calculated with *RADIEL*. The sections of the (100) and (001) planes for (I) and the (110) plane for (II) through the Pd atom are shown in Fig. 1. In Fig. 1(*a*) positive peaks of +2·3 (3) e Å^{-3} are located on the fourfold axis at 0·47 Å from the Pd nucleus, whereas negative troughs of −1·0 (2) e Å^{-3} are located on the Pd—Cl bond axis at 0·36 Å from the Pd nucleus. They indicate excess 4*d* electron population for the a_{1g} (d_{z^2}) orbital and lack of b_{1g} ($d_{x^2-y^2}$) orbital population. In Fig. 1(*b*) there are positive peaks of +0·8 (2) e Å^{-3} on the direction bisecting the Cl—Pd—Cl angle, which show excess 4*d* electron population for the b_{2g} (d_{xy}) orbital. In Fig. 1(*c*) there are positive peaks of +1·4 (3) e Å^{-3} on the

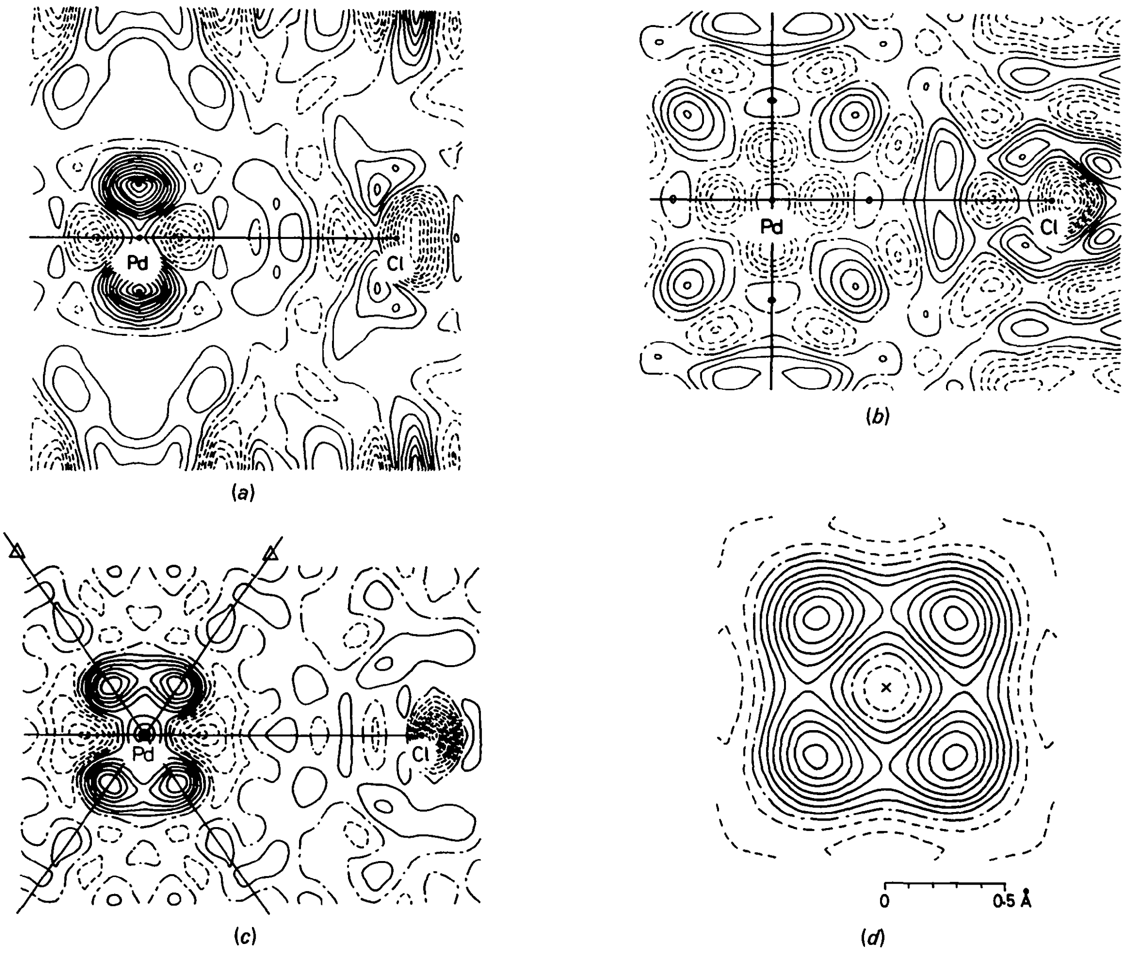

(*a*) (*b*) (*c*) (*d*)

Fig. 1. Deformation densities at 120 K. (*a*) On the (100) plane for (I), (*b*) on the (001) plane for (I), (*c*) on the (110) plane for (II) and (*d*) through the plane perpendicular to the Pd—Cl bond axis at 0·30 Å from the Pd nucleus for (II). The cross indicates the location of the Pd—Cl bond. Contour intervals at 0·2 e Å^{-3}. $\sigma(\Delta\rho) = 0{\cdot}1$ e Å^{-3} except near the atomic nuclei. Negative contours broken, zero contours chain-dotted.

---

* See deposition footnote.

threefold axes at 0·51 Å from the Pd nucleus, and negative troughs of −1·0 (2) e Å^{-3} on the Pd—Cl bond axes at 0·48 Å from the Pd nucleus. They indicate excess 4d electron population for the t_{2g} orbitals and deficiency in the e_g orbitals. Fig. 1(d) shows the section at the face of the cube, on the apices of which the positive deformation density has its maximum (Saito, 1979). This feature is almost the same as that observed for the octahedral complex $[Co(NO_2)_6]^{3-}$ (Ohba, Toriumi, Sato & Saito, 1978). In order to assess the significance of these peaks, their $(\sin\theta/\lambda)_{\max}$ dependence was examined (see Fig. 2). The $(\sin\theta/\lambda)_{\max}$ dependence of the peak heights could be reproduced by simple simulation of the effect of series termination (Lehmann & Coppens, 1977).

Deformation densities at room temperature (see deposition footnote) show similar features: (I) positive peaks of 0·8 (1) e Å^{-3} on the fourfold axes at 0·5 Å from the Pd nucleus, (II) positive peaks of 0·7 (2) e Å^{-3} on the threefold axes at 0·5 Å from the Pd nucleus. The peak positions are almost the same at 300 and 120 K. The peak heights at room temperature are less than half of those at 120 K because of the larger thermal motion. This implies that the charge asphericity is due, not to the thermal vibration of the central metal atom, but to the 4d electrons.

By introducing multipole parameters, the thermal parameters of Pd reduced by 3%, whereas those of the Cl and K atoms were not changed within the standard deviations. The model deformation maps, $\Delta\rho_{\text{model}}$ $(=\rho_{\text{calc,multipole}}-\rho_{\text{calc,spherical}})$ reproduce the aspherical 4d electron distribution: (I) positive peaks 1·5 (3) e Å^{-3} on the fourfold axis at 0·47 Å from Pd nucleus and (II) positive peaks 1·4 (3) e Å^{-3} on the threefold axis at 0·48 Å. For the refinements A, B and C of (I) $\Delta\rho_{\text{model}}$ shows positive peaks at the same position with the same peak heights.

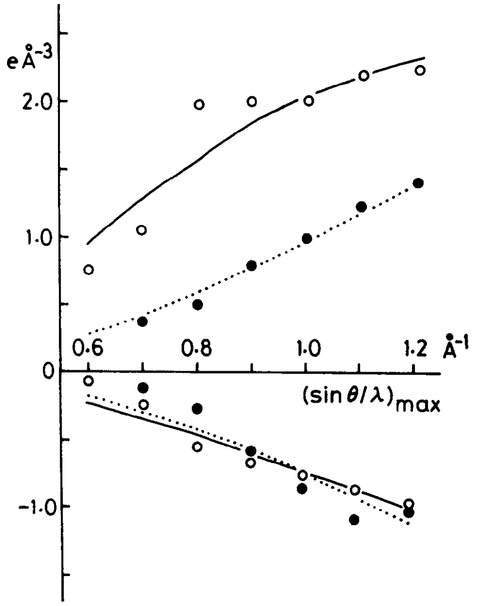

Fig. 2. Peak height of the deformation density as a function of the cut-off value $(\sin\theta/\lambda)_{\max}$ in the Fourier summation. Open and closed circles are observed values for (I) and (II), respectively. Solid and dotted lines are calculated values for (I) and (II).

Table 2. *Electron populations in each of the orbitals of* Pd

	A	B	C
(I)			
b_{1g} $(d_{x^2-y^2})$	1·13 (5)	1·69 (3)	1·49 (1)
b_{2g} (d_{xy})	1·93 (5)	2·25 (3)	2·0
e_g (d_{xz}, d_{yz})	4·49 (6)	4·0	4·0
a_{1g} (d_{z^2})	2·41 (5)	2·0	2·0
Total	9·96 (6)	9·94 (6)	9·49 (3)
(II)			
e_g $(d_{x^2-y^2}, d_{z^2})$	1·89 (7)		
t_{2g} (d_{xy}, d_{xz}, d_{yz})	6·14 (8)		
Total	8·03 (10)		

Refinement A: populations are not constrained; B: populations of a_{1g} and e_g orbitals are fixed; C: populations of a_{1g}, e_g and b_{2g} orbitals are fixed.

The d-orbital populations in Table 2 were calculated with following equations (Holladay, Leung & Coppens, 1983):

(I) D_{4h} symmetry:

$$
\begin{aligned}
P(b_{1g}) &= 0{\cdot}2P_{00} - 1{\cdot}0392P_{20} + 0{\cdot}2326P_{40} + 1{\cdot}5708P_{44}\\
P(b_{2g}) &= 0{\cdot}2P_{00} - 1{\cdot}0392P_{20} + 0{\cdot}2326P_{40} - 1{\cdot}5708P_{44}\\
P(e_g) &= 0{\cdot}4P_{00} + 1{\cdot}0392P_{20} - 1{\cdot}8609P_{40}\\
P(a_{1g}) &= 0{\cdot}2P_{00} + 1{\cdot}0392P_{20} + 1{\cdot}3957P_{40}, \qquad (1)
\end{aligned}
$$

(II) O_h symmetry:

$$
\begin{aligned}
P(e_g) &= 0{\cdot}4P_{00} - 2{\cdot}7914P_{40}\\
P(t_{2g}) &= 0{\cdot}6P_{00} + 2{\cdot}7914P_{40}, \qquad (2)
\end{aligned}
$$

where the P's with parentheses indicate orbital populations and the P_{lm}'s the multipole parameters (deposited). As both (I) and (II) are in the low-spin states, the b_{2g}, e_g and a_{1g} orbitals of (I) and the t_{2g} orbitals of (II) should be fully occupied in the ligand-field approximation with the d^8 and d^6 configuration. The result agrees with this expectation. The populations of (I) b_{1g} and (II) e_g orbitals suggest that the Pd atoms are largely neutralized owing to the coordination of Cl$^-$.

Effective charges of Pd were also estimated by direct integration. The number of electrons in a sphere of radius r centered on the Pd atom, $C(r)$, was calculated. The calculated structure factors of the unobserved reflections with $\sin\theta/\lambda \leq 2$ Å^{-1} were included in the Fourier summation, and for the range of $\sin\theta/\lambda > 2$ Å^{-1} the termination correction was made by the isolated-atom approximation (Kobayashi, Marumo & Saito, 1972). The effective radius of Pd was defined to be 1·2 Å for both complexes based on the minimum of the

Table 3. *Effective charge of* Pd

	Formal	MR[a]	DI[b]	ESCA	NQR
(I)	+2	+0·51 (3)	+0·55 (35)	+0·4 (2)[c]	
(II)	+4	+1·97 (10)	+1·16 (41)	+1·4 (1)[d]	+0·58[e]

Notes: (*a*) multipole refinement [refinement *C* for (I)]; (*b*) direct integration; (*c*) Forkesson & Larsson (1976), $(Ph_4P)_2[PdCl_4]$; (*d*) Larsson & Forkesson (1977), $(Ph_4P)_2[PdCl_6]$; (*e*) Ito, Nakamura, Kurita, Ito & Kubo (1961).

radial distribution, $D(r) = \mathrm{d}C(r)/\mathrm{d}r$. As seen from Fig. 3, $D(r)$ has a shoulder at about 0·5 Å, which corresponds to the 4*d* electrons. The effective charges derived by ESCA and NQR are also listed in Table 3. The counter ion is not K^+ but the tetraphenylphosphonium cation (Ph_4P^+) in the ESCA work. Although the definitions of the effective charge differ from each other, both results suggest that the Pd atoms are considerably neutralized.

In the Fourier synthesis, anomalous dispersion is corrected with the following equation (*International Tables for X-ray Crystallography*, 1974):

$$F_o = \frac{|F_o^a|}{|F_c^a|}A_c + i\frac{|F_o^a|}{|F_c^a|}B_c, \tag{3}$$

where $|F_o^a|$ and $|F_c^a|$ are the observed and calculated structure amplitudes including anomalous dispersion, and F_o and F_c $(= A_c + iB_c)$ are the structure factors for normal scattering. An alternative correction by the following equation has also been proposed (De Titta, 1986):

$$F_o = \left[\frac{|F_o^a|}{|F_c^a|}A_c^a - (A_c^a - A_c)\right] + i\left[\frac{|F_o^a|}{|F_c^a|}B_c^a - (B_c^a - B_c)\right]. \tag{4}$$

For a centrosymmetric structure with the origin at the center of symmetry, the imaginary part of (4) should be zero. The deformation density based on (4) is shown in Fig. 4. In comparison with Fig. 1, the noise level

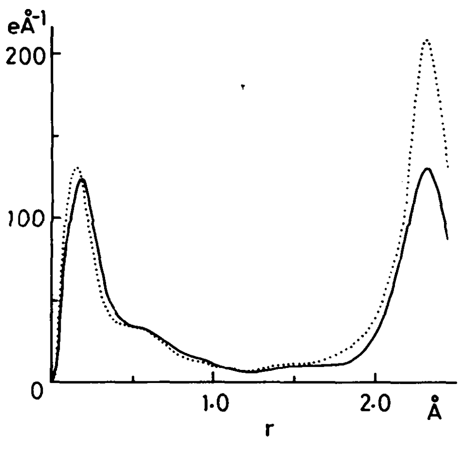

Fig. 3. Radial distribution $D(r) = \mathrm{d}C(r)/\mathrm{d}r$. $C(r)$ is the number of electrons in a sphere of radius *r* centered on Pd. Solid and dotted lines are for (I) and (II), respectively.

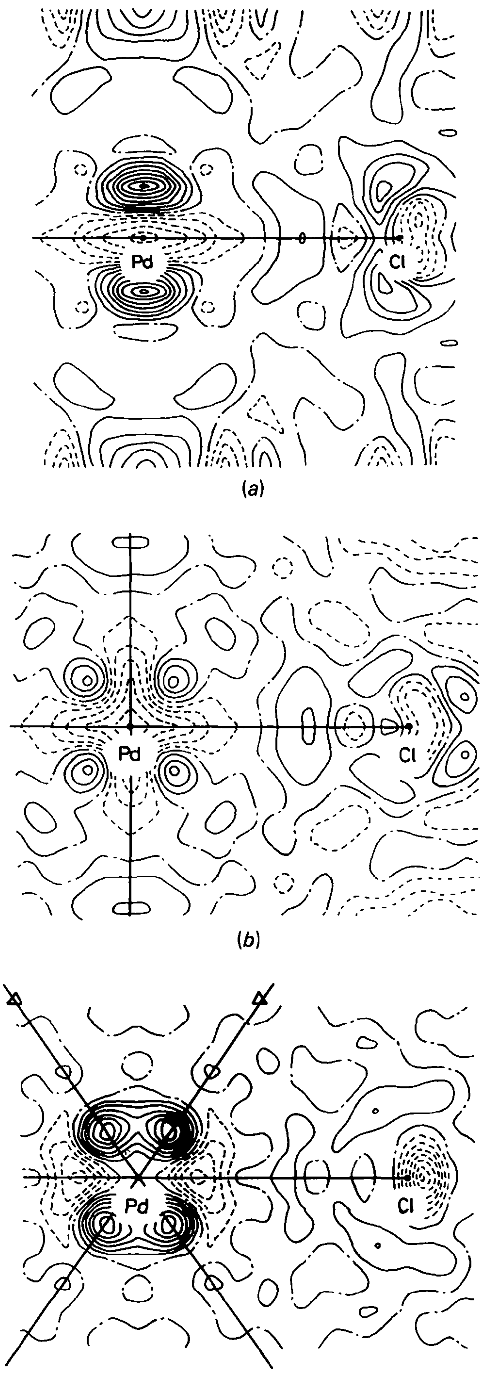

Fig. 4. Deformation densities at 120 K after anomalous-dispersion correction based on the equation (4). (*a*) On the (100) plane for (I), (*b*) on the (001) plane for (I) and (*c*) on the (110) plane for (II). Contour intervals at 0·2 e Å^{-3}. $\sigma(\Delta\rho) = 0·1$ e Å^{-3}.

became lower and the deformation density decreased at the Pd nucleus and increased at the Cl nucleus. However, the charge asphericity due to the $4d$ electrons is not altered drastically. The change in deformation density based on (3) and (4) may be due to a tendency for $|F_o^a|$'s to be slightly larger than $|F_c^a|$'s for the high-order reflections, and to the different sign of $\Delta f'$(Mo $K\alpha$) for Pd and Cl atoms. The error in anomalous-dispersion correction along with the error in scale factor makes the deformation density in the vicinity of the nuclear position of heavy atoms unreliable.

The present study revealed that the very small valence/core electron ratio and large anomalous-dispersion effect of the heavy-metal atoms are not serious problems because the $4d$ electrons are distributed outside the high-density inner-core region and give sharp deformation density.

This work was supported by the research grant of the Foundation 'Hattori Hokokai'.

References

BECKER, P. J. & COPPENS, P. (1975). *Acta Cryst.* A**31**, 417–425.

CLEMENTI, E. & RAIMONDI, D. L. (1963). *J. Chem. Phys.* **38**, 2686–2689.

COPPENS, P., GURU ROW, T. N., LEUNG, P., STEVENS, E. D., BECKER, P. J. & YANG, Y. W. (1979). *Acta Cryst.* A**35**, 63–72.

COPPENS, P. & HALL, M. B. (1982). Editors. *Electron Distributions and the Chemical Bond.* New York: Plenum.

DE TITTA, G. T. (1986). Private communication.

EYRING, H., WALTER, J. & KIMBALL, G. E. (1944). *Quantum Chemistry*, pp. 162–163. New York: John Wiley.

FORKESSON, B. & LARSSON, R. (1976). *Chem. Scr.* **10**, 105–109.

HANSEN, N. K. & COPPENS, P. (1978). *Acta Cryst.* A**34**, 909–921.

HOLLADY, A., LEUNG, P. & COPPENS, P. (1983). *Acta Cryst.* A**39**, 377–387.

International Tables for X-ray Crystallography (1974). Vol. IV. Birmingham: Kynoch Press. (Present distributor Kluwer Academic Publishers, Dordrecht.)

ITO, K., NAKAMURA, D., KURITA, Y., ITO, K. & KUBO, M. (1961). *J. Am. Chem. Soc.* **83**, 4526–4528.

IWATA, M. & SAITO, Y. (1973). *Acta Cryst.* B**29**, 822–832.

KOBAYASHI, A., MARUMO, F. & SAITO, Y. (1972). *Acta Cryst.* B**28**, 2709–2715.

LARSSON, R. & FORKESSON, B. (1977). *Chem. Scr.* **11**, 5–7.

LEHMANN, M. S. & COPPENS, P. (1977). *Acta Chem. Scand. Ser. A*, **31**, 530–534.

OHBA, S. & SAITO, Y. (1984). *Acta Cryst.* C**40**, 1639–1641.

OHBA, S., SATO, S., SAITO, Y., OHSHIMA, K. & HARADA, J. (1983). *Acta Cryst.* B**39**, 49–53.

OHBA, S., TORIUMI, K., SATO, S. & SAITO, Y. (1978). *Acta Cryst.* B**34**, 3535–3542.

SAITO, Y. (1979). *Inorganic Molecular Dissymmetry*, pp. 89–115. Berlin: Springer-Verlag.

TORIUMI, K. & SAITO, Y. (1983). *Electron-Density Distributions in Inorganic Compounds.* New York: Academic Press.

ZACHARIASEN, W. H. (1967). *Acta Cryst.* **23**, 558–564.

Acta Cryst. (1988). B**44**, 585–595

Structurally Based Prediction of Ferroelectricity in Inorganic Materials with Point Group 6*mm*

BY S. C. ABRAHAMS

AT&T Bell Laboratories, Murray Hill, New Jersey 07974, *USA*

(*Received* 9 *May* 1988; *accepted* 11 *August* 1988)

Abstract

Ferroelectricity may be predicted in any pyroelectric crystal that has atomic displacements along the polar axis no greater than about 1 Å from the paraelectric position and in which the largest such displacement is greater than about 0·1 Å. The square of the largest atomic displacement associated with the atoms that form the strongest and least ionic bonds in the structure is proportional to the temperature at which the ferroelectric phase transforms to the paraelectric phase. A systematic approach to ferroelectric prediction, based on these structural principles, is now feasible with the availability of the Inorganic Crystal Structure Database (ICSD) in Karlsruhe. Ferroelectric crystals are generally important technologically more for their optoelectronic properties than for their reversible spontaneous polarization. Two new families of compounds satisfy the structural criteria for ferroelectricity in space group $P6_3cm$ and six families satisfy them in $P6_3mc$; in addition, eight other compounds crystallizing in point group 6*mm* are possibly ferroelectric. Three other families and four additional compounds may be ferroelectric or alternatively may be centrosymmetric. A further thirteen compounds are unambiguously structurally nonpolar. No material reported by ICSD as crystallizing in either space group *P*6*mm* or *P*6*cc* is predicted to be ferroelectric.

Introduction

The study of relationships between the crystal structure of a material and its macroscopic properties is central to the field designated by *Acta Crystallographica* (*Editorial*, 1982) as structural science.

0108-7681/88/060585-11$03.00